

# Resolving isospectral “drums” by counting nodal domains

Sven Gnutzmann<sup>2</sup> ‡, Uzy Smilansky<sup>1</sup>§ and Niels Sondergaard<sup>1</sup>||

<sup>1</sup> Department of Physics of Complex Systems,  
The Weizmann Institute of Science, Rehovot 76100, Israel

<sup>2</sup> Institute for Theoretical Physics,  
Freie Universität Berlin, 14195 Berlin, Germany.

## Abstract.

Several types of systems were put forward during the past decades to show that there exist *isospectral* systems which are *metrically* different. One important class consists of Laplace Beltrami operators for pairs of flat tori in  $\mathbb{R}^n$  with  $n \geq 4$ . We propose that the spectral ambiguity can be resolved by comparing the nodal sequences (the numbers of nodal domains of eigenfunctions, arranged by increasing eigenvalues). In the case of isospectral flat tori in four dimensions - where a 4-parameters family of isospectral pairs is known- we provide heuristic arguments supported by numerical simulations to support the conjecture that the isospectrality is resolved by the nodal count. Thus - one can *count* the shape of a drum (if it is designed as a flat torus in four dimensions...).

## 1. Introduction

Since M. Kac posed his famous question: “can one hear the shape of a drum” [1], the subject of isospectrality appears in many contexts in the physical and the mathematical literature. This question can be cast in a more general way by considering a Riemannian manifold (with or without boundaries) and the corresponding Laplace-Beltrami operator. (Boundary conditions which maintain the self adjoint nature of the operator are assumed when necessary.) Kac’s question is paraphrased to ask “can one deduce the metric of the surface (or the geometry of the boundary) from the spectrum?”. Till today, the answer to this question is not known in sufficient detail. An affirmative answer is known to hold for several classes of surfaces and domains [2, 3, 4] (see also a recent review by S. Zelditch [5]). However, this is not always true. One of the first examples to the negative is due to J. Milnor who proposed in 1964 two flat tori in  $\mathbb{R}^{16}$ , which he proved to be isospectral but not isometric [6]. Since then, many other pairs

‡ Presently on leave at the Department of Physics of Complex Systems,  
The Weizmann Institute of Science, Rehovot 76100, Israel

§ Presently on sabbatical leave at the School of Mathematics, Bristol University, Bristol BS81TW, UK

|| Present address: Division of Mathematical Physics, Lund Institute of Technology Lund University  
Box 118 SE - 221 00 Lund SWEDEN

of isospectral yet not isometric systems were found. M. E. Fisher considered a discrete version of the Laplacian, and gave a few examples of distinct graphs which share the same spectrum [7]. A general method for constructing isospectral, non-isometric manifolds has been designed by T. Sunada [10]. Sunada’s technique applies also to discrete graphs [11], and the late Robert Brooks [11], gave a few examples of families of non-Sunada discrete graphs. Sunada’s method was also used by Gordon *et. al.* [8] and Chapman [9] to construct isospectral domains in  $\mathbb{R}^2$ . Other pairs of isospectral domains in  $\mathbb{R}^2$  were proposed in [13] and discussed further in [14]. Sunada-like quantum graphs were presented in [4].

Milnor’s original work on isospectral flat tori in  $\mathbb{R}^{16}$  induced several investigators to find other examples in spaces of lower dimensions. Kneser [15] constructed an example in dimension  $n = 12$ , and proved that there exist no such pair in two dimensions. Wolpert [16] showed that all sets of mutually isospectral but non-isometric flat tori are finite at any dimension. The first examples in dimension  $n = 4$  were found by Schiemann [12], and later by Earnest and Nipp [17]. These results were generalized by Conway and Sloane [18], who constructed sets of isospectral pairs of flat tori in  $n = 4, 5, 6$ , and these sets depend continuously on several parameters.

The existence of such a large variety of isospectral pairs, suggests naturally the question - what is the additional information necessary to resolve the isospectrality. We would like to propose that this information is stored in the sequences of nodal counts, defined as follows. Consider only real eigenfunctions of the Laplace-Beltrami operator and assign to each eigenfunction the number of its connected domains where the eigenfunction does not change its sign (such a domain is a nodal domain). The nodal sequence is obtained by arranging the number of nodal domains by the order of increasing eigenvalues. Sturm’s oscillation theorem in one dimension, and Courant’s generalization to higher dimensions express the intimate relation between the nodal sequence and the corresponding spectrum. However, the information stored in the nodal sequence and in the spectrum is not the same, and here we would like to propose that the additional knowledge obtained from the nodal sequence can resolve isospectrality. We address in particular isospectral flat tori in four dimensions of the type mentioned above. The simplicity of the geometry, together with the rich variety of pairs, make this class of systems very convenient, especially here, when the approach is explored for the first time.

The paper is organized as follows. In section (2) we shall summarize some of the properties of flat tori, their spectra and eigenfunctions. The fact that the spectra are highly degenerate requires a special choice of the basis set of wave functions for which the nodal domains are to be counted. The quantity which signals the difference between the isospectral tori is defined in subsection (3.1). The arguments which lead us to suggest that this quantity resolves isospectrality are explained for the families of flat tori in four dimensions [18], and it is presented in subsection (3.2). A summary and some concluding remarks will be given in the last section.

## 2. Flat Tori

A flat torus is a Riemannian manifold which is a quotient of  $\mathbb{R}^n$  by a lattice of maximum rank:  $T = \mathbb{R}^n / A\mathbb{Z}^n$ , where  $A = (\mathbf{g}^{(1)}, \dots, \mathbf{g}^{(n)})$ . Thus, the lattice  $A\mathbb{Z}^n$  is spanned by the  $\mathbf{g}^{(r)}$ . The reciprocal lattice will be denoted by  $\hat{\mathbf{g}}^{(r)}$ , and  $(\hat{\mathbf{g}}^{(s)} \cdot \mathbf{g}^{(r)}) = \delta_{r,s}$ . The Gram matrices for the lattice will be denoted by  $G = A^\top A$ , and its reciprocal will be denoted for brevity by  $Q = G^{-1} = (A^{-1})(A^{-1})^\top$ . In the present work we shall deal with dimensions  $n \geq 4$ . We shall assume throughout that the lattice vectors  $A$  cannot be partitioned to mutually orthogonal subsets.

### 2.1. Spectra

We are interested in the spectrum of the Laplace Beltrami operator  $\Delta = -\sum_{i=1}^n \frac{\partial^2}{\partial x_i^2}$  with eigenfunctions which are uniquely defined on  $T$ . They can be explicitly written down as:

$$\Psi_{\mathbf{q}}(\mathbf{x}) = \exp\left(2\pi i \sum_{r=1}^n q_r (\hat{\mathbf{g}}^{(r)} \cdot \mathbf{x})\right) \quad (1)$$

where  $\mathbf{q} = (q_1, \dots, q_n) \in \mathbb{Z}^n$ ,  $\mathbf{x} \in T$ . The corresponding eigenvalues are

$$E_{\mathbf{q}} = (2\pi)^2 (\mathbf{q} \cdot Q \mathbf{q}). \quad (2)$$

The spectrum of a flat torus may be degenerate, and we denote the degeneracy by

$$g_Q(E) = \#\{\mathbf{q} \in \mathbb{Z}^n : E = E_{\mathbf{q}}\} . \quad (3)$$

If the matrix elements of  $Q$  are *rational*, it is convenient to express the energy in units of  $(2\pi)^2/l(Q)$  where  $l(Q)$  is the least common denominator of the elements of  $Q$ . In these units the energy values are integers, and  $g_Q(E)$  equals the number of times that  $E$  can be represented as an integer quadratic form. The integer vectors which satisfy (2) will be called *representing vectors* in the sequel. Their tips are points on the  $n$  dimensional ellipsoid (2), and their distribution on the ellipsoid will be discussed in the sequel. The study of the spectrum (i.e. those integers that can be represented by a given integer quadratic form) and the degeneracies (the number of representations) is a subject which was studied at length in number theory. Here, we shall give a brief summary of the results which are essential for the present work. The interested reader is referred to [19, 20] for further references and details.

(a) For integer  $Q$ , the eigenvalues are integers  $E$  which must satisfy the congruence

$$E = m \pmod{c(Q)} ; \quad m \in \mathbb{N} \quad (4)$$

and  $c(Q)$  is an integer which depends on  $Q$ . This result implies that the spectrum is *periodic*.

(b) The degeneracy  $g_Q(E)$  for *integer*  $Q$  increases as  $E^{\frac{n}{2}-1}$ . This estimate can be derived by a simple heuristic argument. The number of integer grid points in a shell of width

$\delta E$  is proportional to  $E^{\frac{n-1}{2}} \delta E / E^{\frac{1}{2}}$ . If  $Q$  is integer,  $E$  must be an integer, and hence, the number of values it can take in the interval of interest is  $\delta E$ . Thus,

$$g_{\text{rat}}(E) \sim \frac{\# \text{ grid points}}{\# \text{ possible values}} \propto E^{\frac{n}{2}-1}. \quad (5)$$

From (a) and (b) above, it follows that not all integers appear in the spectrum, and the gaps are determined by the gaps which appear in the first  $c(Q)$  eigenvalues in the spectrum. The distribution of the gap sizes may be very complex, and depend delicately on  $Q$ . Still, one can define the mean gap size, and this value applies for the entire spectrum.

(c) For *irrational* matrices of the form  $Q = Q_0 + \alpha Q_1$  where  $Q_0, Q_1$  are both integer, and  $\alpha$  is irrational, the mean degeneracy increases more slowly with  $E$ , namely,  $g(E) \propto E^{\frac{n}{2}-2}$ . Here, the degeneracy class consists of the grid points which satisfy both  $E_0 = \mathbf{q} \cdot Q_0 \mathbf{q}$  and  $E_1 = \mathbf{q} \cdot Q_1 \mathbf{q}$  with  $E = E_0 + \alpha E_1$ , and both  $E_0$  and  $E_1$  integers. Their number is proportional to the volume of the intersection of the corresponding ellipsoid shells  $E^{\frac{n-2}{2}} \delta E_0 \delta E_1 / (E_0 E_1)^{\frac{1}{2}}$ . The number of spectral values is now the number of integer points in the square of size  $\delta E_0 \delta E_1$ . Thus, in the irrational case,

$$g_{\text{irrat}}(E) \propto E^{\frac{n}{2}-2}. \quad (6)$$

Figure 1. shows the dependence of the mean value of  $g(E)$ , averaged over the eigenvalues  $E_i$  in an interval of width  $\Delta E$  centered at  $E$ ,

$$\langle g(E) \rangle = \frac{1}{M} \sum_{i: |E_i - E| < \Delta E / 2} g(E_i). \quad (7)$$

$M$  stands for the number of eigenvalues in the interval. The linear dependence of  $\langle g(E) \rangle$  at sufficiently large  $E$  for rational  $Q$  and its independence of energy in the irrational case are clearly illustrated.

(d) For integer  $Q$ ,  $n \geq 4$  and in the limit of large  $E$ , the representing integer vectors of  $E$  are uniformly distributed on the ellipsoid: Given a well behaved function  $f(\mathbf{x})$  on the unit ellipsoid  $\mathcal{E} = \{\mathbf{x} \in \mathbb{R}^n : \mathbf{x} \cdot Q \mathbf{x} = 1\}$ ,

$$\lim_{E \rightarrow \infty} \frac{1}{g(E)} \sum_{\mathbf{q}: Q \mathbf{q} = E} f\left(\frac{\mathbf{q}}{\sqrt{E}}\right) - \int_{\mathcal{E}} f(\mathbf{x}) d\mathbf{x} = 0. \quad (8)$$

## 2.2. Isospectral flat tori in four dimensions

To end this section, we shall describe the 4-parameter family of non isometric yet isospectral flat tori which is the system we shall consider in most of the examples to be discussed in the sequel. This family which was discovered by J. H. Conway and N. J. A. Sloane [18] includes, as a particular case, the previously known example of Schiemann [12]. Their spectra are given explicitly by the pairs of positive definite matrices, which depend on the 4 positive parameters  $a, b, c, d$ :

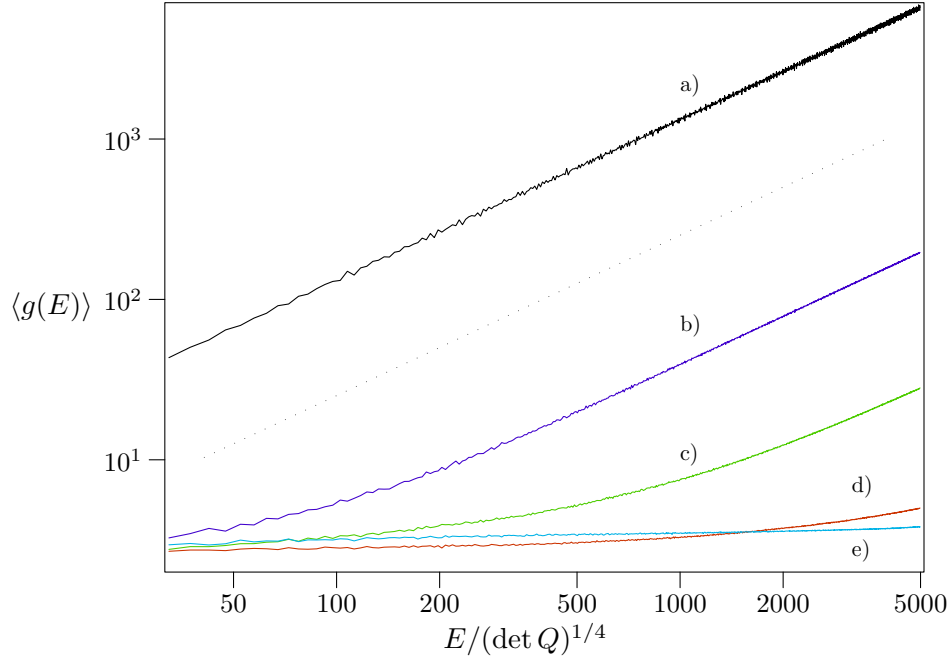


**Figure 1.** Double logarithmic plot of the spectral averaged degeneracy (7). The five data sets correspond to: a)  $\beta = 2$ , b)  $\beta = 3/2$ , c)  $\beta = 5/3$ , d)  $\beta = 8/5$  and e)  $\beta = (\sqrt{5}+1)/2$ . a)-d) correspond to integer tori and e) to an irrational. The parameter  $\beta$  is explained in the text at the end of section 2.2. The dotted line is a linear function of  $E$  included for comparison.

$$Q^+ = \frac{1}{12} \begin{pmatrix} 9a + b + c + d & 3a - 3b - c + d & 3a + b - 3c - d & 3a - b + c - 3d \\ 3a - 3b - c + d & a + 9b + c + d & a - 3b + 3c - d & a + 3b - c - 3d \\ 3a + b - 3c - d & a - 3b + 3c - d & a + b + 9c + d & a - b - 3c + 3d \\ 3a - b + c - 3d & a + 3b - c - 3d & a - b - 3c + 3d & a + b + c + 9d \end{pmatrix} \quad \text{and} \quad (9)$$

$$Q^- = \frac{1}{12} \begin{pmatrix} 9a + b + c + d & -3a + 3b - c + d & -3a + b + 3c - d & -3a - b + c + 3d \\ -3a + 3b - c + d & a + 9b + c + d & a + 3b - 3c - d & a - 3b - c + 3d \\ a + b + 3c - d & a + 3b - 3c - d & a + b + 9c + d & a - b + 3c - 3d \\ -3a - b + c + 3d & a - 3b - c + 3d & a - b + 3c - 3d & a + b + c + 9d \end{pmatrix}.$$

Several properties of these matrices can be derived by straightforward computations:

*i.* The spectra of  $Q^+$  and  $Q^-$  are identical, and consist of the values  $a, b, c, d$ . The unitary matrices which bring  $Q^\pm$  to diagonal form are *independent* of the parameters. Explicitly

$$D \equiv \text{diag}\{a, b, c, d\} = T^\pm Q^\pm (T^\pm)^\top \quad (10)$$

$$T^\pm = \frac{1}{\sqrt{12}} \left[ \begin{pmatrix} 0 & 1 & 1 & 1 \\ -1 & 0 & -1 & 1 \\ 1 & -1 & 0 & 1 \\ 1 & 1 & -1 & 0 \end{pmatrix} \pm 3 \begin{pmatrix} 1 & 0 & 0 & 0 \\ 0 & 1 & 0 & 0 \\ 0 & 0 & -1 & 0 \\ 0 & 0 & 0 & -1 \end{pmatrix} \right].$$

ii.  $Q^+$  and  $Q^-$  commute only when at least three of the parameters  $a, b, c, d$  are equal. From now on when we shall refer to the four parameters family of isospectral tori, we shall exclude this set which represents ellipsoids with cylindrical or spherical symmetry.

iii. The unitary matrix  $U$  which transform  $Q^+$  to  $Q^-$ ,  $Q^- = U^\top Q^+ U$  is *independent* of the parameters  $a, b, c, d$ ,

$$U = (T^+)^{\top} T^- = \frac{1}{2} \begin{pmatrix} -1 & 1 & 1 & 1 \\ -1 & -1 & -1 & 1 \\ -1 & 1 & -1 & -1 \\ -1 & -1 & 1 & -1 \end{pmatrix} ; \quad \det U = 1 . \quad (11)$$

Consider an integer vector  $\mathbf{q}$  with  $\mathbf{q} \cdot Q^- \mathbf{q} = E$ .  $U\mathbf{q}$  is on the ellipsoid generated by  $Q^+$ , but it is *integer* only if  $\sum_{i=1}^4 |q_i|$  is even. In this case, also  $\sum_{i=1}^4 |(U\mathbf{q})_i|$  is even. Hence, integer vectors with *even sums* map to each other under  $U$ . The integer vectors with *odd sums* do not have this property.

Conway and Sloane’s paper offers another family of isospectral tori in four dimensions. This is a two parameter family which we shall not discuss in detail, although the numerical results obtained for this case support the conclusions derived from the study of the four parameters family.

To end this section we would like to describe the numerical simulations which accompany the subsequent discussions. We have calculated the first 120 million eigenvalues for five pairs of isospectral tori (together with the corresponding nodal sequences defined in the next section). Four of the pairs have been chosen rational, one irrational. The four parameters that define a pair (see eq. (9)) are all of the form  $(a, b, c, d) = (\alpha, \alpha/\beta^2, \alpha/\beta^4, \alpha/\beta^6)$ . Here  $\alpha$  just rescales the spectrum, for the rational tori it is taken such that the tori are actually integer. For the irrational pair it has been set to  $\alpha = 1$ . Note, that we present all results as a function of  $E/(\det Q)^{1/4}$  which is invariant under rescalings of the spectrum. For the other parameter we have chosen the five values  $\beta_i = 2, 3/2, 5/3, 8/5, (\sqrt{5} + 1)/2$ . The latter value defines the irrational pair ( $\beta_5 = (\sqrt{5} + 1)/2$  is the golden ratio), the other parameters are rational approximants to the golden ratio along the Fibonacci sequence. Integer tori are obtained by setting  $\alpha_i = 2^8, 2^2 \times 3^7, 3 \times 5^6, 2^{20}$  (which results in  $\det Q(\alpha_i, \beta_i) = 2^{20}, 3^{16} \times 2^{20}, 3^{16} \times 5^{12}, 2^{44} \times 5^{12}$ ).

### 3. Nodal domains and isospectrality

In this section we shall define the nodal sequences of the flat tori under consideration, and will show how they can resolve isospectrality.

To define the nodal domains, we consider the real counterparts of (1),

$$\Psi_{\mathbf{q}}^{(+)} = \cos \left( 2\pi \sum_{r=1}^n q_r (\hat{\mathbf{g}}^{(r)} \cdot \mathbf{x}) \right) \quad ; \quad \Psi_{\mathbf{q}}^{(-)} = \sin \left( 2\pi \sum_{r=1}^n q_r (\hat{\mathbf{g}}^{(r)} \cdot \mathbf{x}) \right) \quad (12)$$

and to avoid double counting, we must exclude  $-\mathbf{q}$  if  $\mathbf{q}$  is included.

A convenient representation can be obtained by the transformation

$$\mathbf{y} = G\mathbf{x} \quad ; \quad \mathbf{x} \in T \quad , \quad \mathbf{y} \in T_y = \mathbb{R}^n / \mathbb{Z}^n \quad (13)$$

so that

$$\Delta_y = - \sum_{r,s=1}^n Q_{r,s} \frac{\partial^2}{\partial y_r \partial y_s} \quad (14)$$

and

$$\Psi_{\mathbf{q}}^{(+)}(\mathbf{y}) = \cos(2\pi(\mathbf{q} \cdot \mathbf{y})) \quad ; \quad \Psi_{\mathbf{q}}^{(-)}(\mathbf{y}) = \sin(2\pi(\mathbf{q} \cdot \mathbf{y})) \quad . \quad (15)$$

From this representation it is evident that as long as the lattice vectors cannot be reduced to mutually orthogonal subspaces, the *real* wave functions cannot be expressed in a product form. The number of nodal domains is defined by lifting the wave functions to  $\mathbb{R}^n$  and counting their nodal domains in the unit cell. The nodal domains form parallel strips separated by  $n-1$  dimensional nodal hyper-planes. The number of nodal domains is

$$\hat{\nu}[\mathbf{q}] = 2 \sum_{r=1}^n |q_r| \quad . \quad (16)$$

This result can be proved by induction, and we start by assuming that all the  $q_i$  are positive. (16) is trivially true for  $n=1$ , where the nodal manifold are points. In 2-d, the nodal manifold are lines which are perpendicular to the direction  $(q_1, q_2)$ . There are  $2q_1$  such lines which intersect the unit interval on the  $y_1$  axis at the points which are the nodal manifolds of the 1-d problem. There are additional  $2q_2 - 1$  lines which intersect the interval  $1 < y_2 < 1$  on the line  $y_1 = 1$ . In total there are  $2(q_1 + q_2) - 1$  nodal lines in the unit interval and therefore  $2(q_1 + q_2)$  nodal domains. The same argument can now be repeated for any  $n$ . The case when some  $q_i$  are negative can be taken care of by a proper reflection. It is also clear that the number of nodal domains of any linear combination of  $\Psi_{\mathbf{q}}^{(+)}(\mathbf{y})$  and  $\Psi_{\mathbf{q}}^{(-)}(\mathbf{y})$  (12) depends on  $\mathbf{q}$  only.

The strip structure discussed above is very different from the morphology of nodal domains in *separable* systems, which are formed from intersections of locally perpendicular hyper-planes.

The special feature of the flat tori to be discussed here is that their spectra are degenerate, and the degeneracies are maximal when the tori are integer. Any linear combination of the eigenfunctions in the degenerate space is itself an eigenfunction, and its nodal structure may depend on the particular combination. To be definite, we must chose a unique representation of the wave functions, for which the nodal count can be defined in an unambiguous way. For this purpose we require that the eigenfunctions are presented in the form of a single term and the nodal domains are parallel strips in the

unit cell. This definition singles out a well defined basis for each degeneracy space, and the number of nodal domains is given by (16).

### 3.1. Counting nodal domains

In a previous work [22], we have shown that counting nodal domains can reveal important information concerning the classical dynamics of the system under study. In particular, arranging the spectrum by increasing values of the eigenvalues, we studied the distribution of the normalized nodal counts  $\xi_n = \frac{\hat{\nu}_n}{n}$ , where  $\hat{\nu}_n$  is the number of nodal domains of the  $n$ 'th wave function. Courant's theorem guaranties that  $\xi_n \leq 1$ . The  $\xi$  distributions have characteristic and universal form if the problem is separable, which is distinct from the distribution which prevails when the classical dynamics is chaotic.

As long as the degeneracy in the spectrum is accidental, one can ignore the ambiguity induced in the ordering of the spectrum by the degeneracy. In the present case, the degeneracy increases as a power of  $E$ , and therefore a different quantity, which is independent of the ordering of the wave functions within a degeneracy subspace, is called for.

A natural modification of the normalized nodal counts for a highly degenerate spectrum is obtained by considering the quantity

$$\nu_Q(E) = \frac{1}{g_Q(E)} \sum_{\mathbf{q} \in \mathbb{Z}^n: E = \mathbf{q} \cdot Q \mathbf{q}} \hat{\nu}[\mathbf{q}] = \frac{1}{g_Q(E)} \sum_{\mathbf{q} \in \mathbb{Z}^n: E = \mathbf{q} \cdot Q \mathbf{q}} \left[ 2 \sum_{i=1}^n |q_i| \right]. \quad (17)$$

We shall refer to  $\nu_Q(E)$  as the *nodal count* associated with the degenerate eigenvalue  $E$ . It coincides with the standard definition for non degenerate cases. The nodal count is the tool by which we propose to resolve isospectrality. It is defined as an average over the representing vectors on the surface of the ellipsoid  $E = \mathbf{q} \cdot Q \mathbf{q}$ . Because of (8), the mean value of  $\nu_Q(E)$  for large  $E$  assumes a well defined, and geometrically appealing value.

### 3.2. Nodal counts and isospectrality

In this section we shall summarize the evidence we have in support of the conjecture that the sequences of nodal counts of tori which are isospectral but not isometric are different. Denoting by  $Q^+$  and  $Q^-$  the corresponding pair of Gramm matrices, and by  $E$  a spectral point, we study the difference

$$\delta\nu(E) = \nu_{Q^+}(E) - \nu_{Q^-}(E). \quad (18)$$

Rather than examining (18) for individual eigenvalues, we shall consider its average over spectral intervals, and the fluctuations about the mean.

Using the fact that in the limit of large  $E$  the representation vectors are distributed homogeneously over the ellipse (8), we get,

$$\langle \nu_Q(E) \rangle \propto E^{\frac{1}{2}} \int_{\mathbb{R}^4} d\mathbf{s} \delta(1 - \mathbf{s} \cdot Q \mathbf{s}) \hat{\nu}[\mathbf{s}]$$



$$= E^{\frac{1}{2}} \int_{\mathbb{S}^3} \frac{d\boldsymbol{\omega} \hat{\nu}[\boldsymbol{\omega}]}{(\boldsymbol{\omega} \cdot Q \cdot \boldsymbol{\omega})^{5/2}}, \quad (19)$$

where the factor  $E^{\frac{1}{2}}$  is due to the linear dependence of  $\hat{\nu}[\mathbf{q}]$  on  $\mathbf{q}$ . We use this expression to prove that  $\langle \delta\nu(E) \rangle = 0$ . This is trivially true for  $a = b = c = d$ , where the two ellipsoids degenerate to a sphere. In Appendix A we show this in general, i.e. the smooth nodal counts agree. The numerical simulations reproduce this behavior, and we use this fact as a check of the numerical procedure.

The fluctuations in the difference of the nodal sequences are best demonstrated by studying the variance

$$\langle (\delta\nu(E))^2 \rangle = \frac{1}{M} \sum_{|E-E_m| < \Delta/2} (\nu_{Q^+}(E_m) - \nu_{Q^-}(E_m))^2; \quad E_m \text{ in the spectrum.} \quad (20)$$

Here  $\Delta \ll E$  and  $M = \#\{E_m : |E - E_m| < \Delta/2\}$ . The variance  $\langle (\delta\nu(E))^2 \rangle$  was computed for the examples of non isometric yet isospectral tori discussed in conjunction with figure 1. The results are shown in Figure 2. The variance does not vanish, and its  $E$  dependence clearly distinguishes between the rational and irrational pairs. It shows the variance for the isospectral tori which were introduced at the end of section (2.2). The two extreme values ( $\beta = 2$  and  $\beta = (\sqrt{5} + 1)/2$ ) show the expected dependence on  $E$  over the entire range of  $E$  values. The data for the intermediate sets of parameters follow the expected asymptotic behavior only after  $E$  is large enough to “distinguish” that the coefficients are rational. The same behavior was also observed for the two parameter family of isospectral tori in four dimensions mentioned in [18].

We are unable to prove that the variance (20) differs from zero, and that its  $E$  dependence follows the behavior expected from the numerical simulations. However, we can provide heuristic arguments which explain the systematic trends observed in the data. The underlying assumptions are that

I. The number of nodal domains for individual representing vectors  $\hat{\nu}[\mathbf{q}] = 2 \sum_{r=1}^n |q_r|$  (16) fluctuate independently about their mean (19).

II. The fluctuations in  $\delta\nu_{Q^+}(E)$  and  $\delta\nu_{Q^-}(E)$  are also independent. (This is supported by the observation made in point *iii.* of the preceding section, that only a fraction of the representation vectors of the two Gram matrices can be transformed to each other by a single rotation.)

The first assumption together with the central limit theorem leads to the conclusion that

$$\langle (\nu_{Q^+}(E) - \langle \nu_{Q^+}(E) \rangle)^2 \rangle \propto \frac{E}{\langle g_{Q^+}(E) \rangle}. \quad (21)$$

The factor  $E$  in the numerator comes because the nodal count scales as  $E^{\frac{1}{2}}$ . The denominator  $\langle g_{Q^+}(E) \rangle$  is the mean number of integer points on the ellipsoid. This behavior is consistent with recent number theoretical estimates of the rate of convergence of the fluctuations of the distribution of representations to the uniform limit [21]. Using the second assumption, we conclude that

$$\langle (\delta\nu_{Q^+}(E))^2 \rangle \propto \frac{E}{\langle g_{Q^+}(E) \rangle} \quad (22)$$

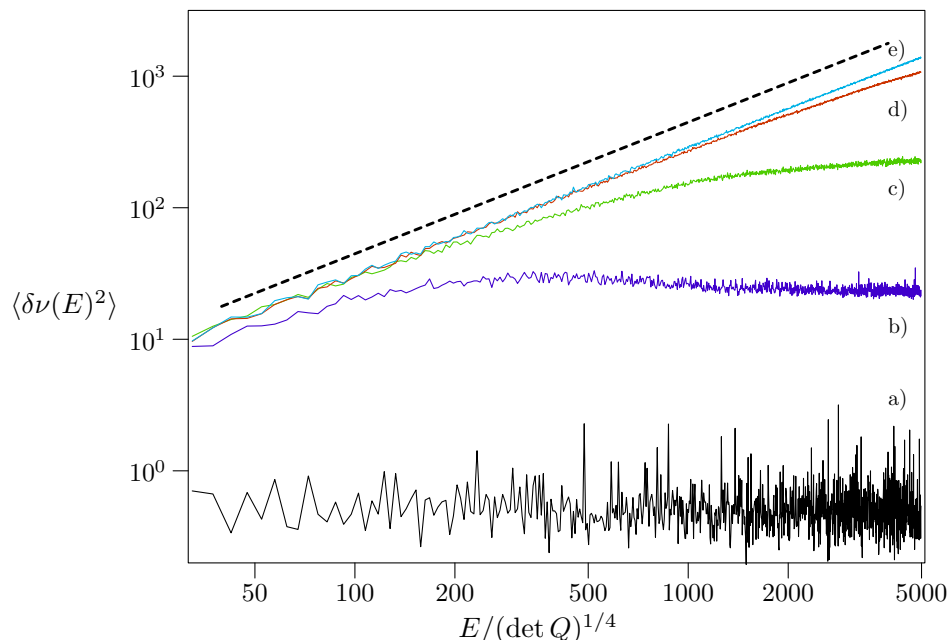


**Figure 2.** Double logarithmic plot of the variance  $\langle \delta\nu(E)^2 \rangle$  (20). The parameters are the same as in figure 1. The dashed line is a linear function of  $E$  included for comparison.

Thus, for *rational*  $Q^\pm$  where  $\langle g_Q(E) \rangle \propto E$ , the variance is independent of  $E$ , whereas for *irrational*  $Q^\pm$  the variance is expected to vary linearly with  $E$ . This behavior is indeed observed in the numerical simulations.

Another numerical test which supports the validity of the above analysis, consisted in computing the fluctuations of the integrated nodal counts

$$N_Q(E) = \frac{1}{\mathcal{N}(E)} \left( \sum_{\mathbf{q} \in \mathbb{Z}^n: \mathbf{q} \cdot Q \mathbf{q} \leq E} \hat{\nu}[\mathbf{q}] \right), \quad (23)$$

where  $\mathcal{N}(E) \sim E^2$  is the spectral counting function  $\mathcal{N}(E) = \sum_{e \leq E} g_Q(e)$ . The difference between integrated nodal counts for the isospectral pair can be written as

$$\Delta N(E) = N_{Q^+}(E) - N_{Q^-}(E) = \frac{1}{\mathcal{N}(E)} \left( \sum_{\mathbf{q} \in V_+} \hat{\nu}[\mathbf{q}] - \sum_{\mathbf{q} \in V_-} \hat{\nu}[\mathbf{q}] \right), \quad (24)$$

where  $V_\pm := \{\mathbf{q} \in \mathbb{Z} : \mathbf{q} \cdot Q_\pm \mathbf{q} \leq E \text{ and } \mathbf{q} \cdot Q_\mp \mathbf{q} > E\}$ . Here, we made use of the exact cancellations of the contributions of  $\mathbf{q} \in \mathbb{Z}$  in the intersection of the two ellipsoids  $\mathbf{q} \cdot Q_+ \mathbf{q} \leq E$  and  $\mathbf{q} \cdot Q_- \mathbf{q} \leq E$ . There are further exact cancellations since  $\hat{\nu}[\mathbf{q}]$  is invariant under reflections  $q_i \rightarrow -q_i$  and due to the symmetries between the two ellipsoids. Assuming that uncorrelated contributions to  $\Delta N(E)$  stem from a thin layer at the surface of the two ellipsoids while bulk contributions cancel we have a sum over  $s \sim |\mathbf{q}|^3 = E^{3/2}$  independent contributions of order  $\hat{\nu}[\mathbf{q}] \sim E^{1/2}$  that vanishes in the mean. For the variance this assumption leads to  $\langle N_Q(E)^2 \rangle \sim \frac{s \hat{\nu}[\mathbf{q}]^2}{\mathcal{N}(E)^2} \sim E^{-3/2}$  in

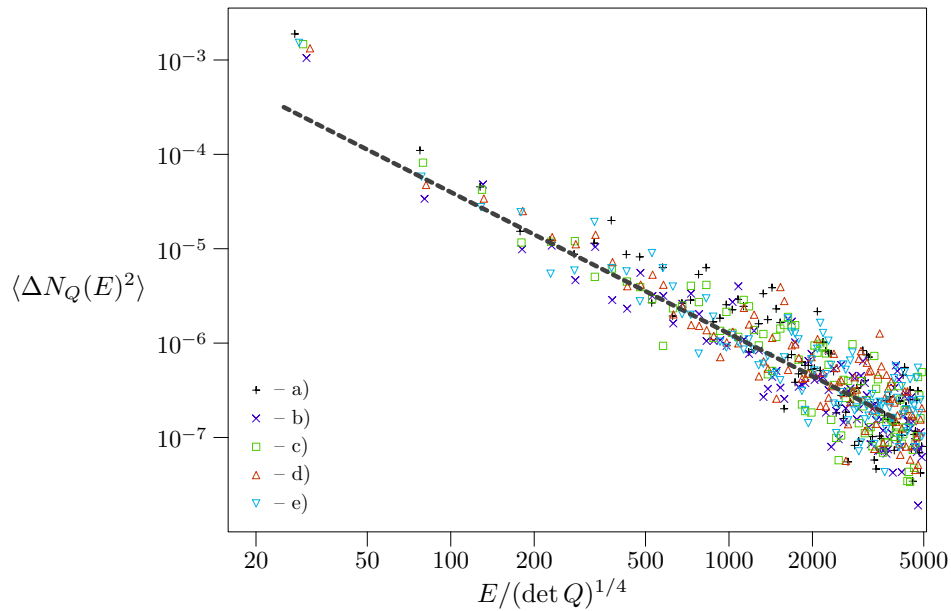


**Figure 3.** Double logarithmic plot of the squared nodal count difference  $\langle \Delta N(E)^2 \rangle$  (smoothed by taking an average over a small spectral interval  $\Delta E$ ). The parameters are the same as for figure 1. The dotted line shows the theoretical prediction  $E^{-3/2}$ .

accordance with our numerical analysis (see figure 3). Note, that this result is valid for both, rational and irrational tori.

#### 4. Summary and conclusions

The heuristic arguments as well as the numerical evidence collected above, support our conjecture that isospectral flat tori can be distinguished by studying the fluctuations of their nodal counts. A formal proof is still lacking. At the same time, the work indicates a hitherto unnoticed link between isospectrality and nodal counts. We hope that the present work will induce more research effort in this direction.

The nodal count studied here is a particular function of the representation vectors whose fluctuations distinguish between the isospectral tori. Are there any other functions which are sensitive to these differences? We investigated this question to some extent, and were not able to find a simple criterion which the function should satisfy in order to resolve the spectral ambiguity. The nodal count was not chosen arbitrarily, and it is rewarding that it does have the required property.

As was mentioned above, there exist several other known families of flat tori beyond the ones discussed here at length. The way of reasoning proposed above should apply to these cases as well. Exploratory work in this direction shows that the nodal sequences of isospectral pairs are different for the cases that were tried, but a systematic study gets prohibitively time consuming as the dimension increases.

The conjecture that nodal counts resolve isospectrality is now being tested for

a different class of operators - the Schrödinger operators on quantum graphs [23]. Preliminary results support the validity of the conjecture also for this class of operators which are quite different from the flat tori discussed here.

## 5. Acknowledgments

This work was supported by the Minerva Center for non-linear Physics, the Einstein (Minerva) center at the Weizmann Institute and by ISF and GIF research grants. NS acknowledges a post doctoral fellowship from the European Network on *Mathematical aspects of Quantum Chaos* which supported his stay at the Weizmann Institute. US acknowledges support from the EPSRC grant GR/T06872/01. We would like to thank Professor Zeev Rudnick for several crucial comments and discussions.

## Appendix A. The mean nodal counts of isospectral tori

To demonstrate the equality of the smooth parts consider the simpler quantity

$$\tau_Q = \int_{\mathbb{S}^3} d\boldsymbol{\omega} \sum_i |\omega_i| \cdot \frac{1}{(\boldsymbol{\omega} \cdot Q \cdot \boldsymbol{\omega})^\eta} \quad (\text{A.1})$$

with  $\eta$  some power e.g.  $5/2$ . The goal is to show  $\tau_{Q^+} = \tau_{Q^-}$ . From the diagonalization (10):

$$Q^\pm = (T^\pm)^\top D T^\pm \quad (\text{A.2})$$

make a change of variables

$$\mathbf{o} = T^\pm \cdot \boldsymbol{\omega} . \quad (\text{A.3})$$

This preserves the measure as  $T^\pm$  are orthogonal and the denominators are seen to agree as  $D$  is the same for the two lattices. The numerator becomes

$$\sum_i |\omega_i| = \sum_{i,j} |(T^\pm)_{ij}^\top o_j| = \sum_{i,j} |T_{ji}^\pm o_j| . \quad (\text{A.4})$$

By explicit calculation we get for the “+” lattice:

$$\begin{aligned} \sqrt{12} \sum_i |\omega_i| &= |o_1 + o_2 + o_3 - 3o_4| + |o_1 - o_2 - 3o_3 - o_4| \\ &\quad + |o_1 + 3o_2 - o_3 + o_4| + |3o_1 - o_2 + o_3 + o_4| , \end{aligned} \quad (\text{A.5})$$

and similarly for the “-” lattice,

$$\begin{aligned} \sqrt{12} \sum_i |\omega_i| &= |o_1 - o_2 + 3o_3 - o_4| + |o_1 - 3o_2 - o_3 + o_4| \\ &\quad + | - 3o_1 - o_2 + o_3 + o_4| + |o_1 + o_2 + o_3 + 3o_4| . \end{aligned} \quad (\text{A.6})$$

Each absolute value for one lattice can be made to correspond to the other under the change of  $o_i$  to  $-o_i$ . For instance the first term of the “+” lattice matches with the fourth of the “-” lattice. In the integral for  $\tau$  such sign changes preserve both the integration domain, the measure and the denominator. Therefore when splitting the

integral into four, corresponding to the terms of (A.5,A.6), each of these terms can be brought to an agreement.

### Bibliography

- [1] M. Kac, Amer. Math. Monthly, **73** (1966) 1-23.
- [2] J. Brüning and E. Heintze, Math. Ann. **269**, 95 (1984).
- [3] S. Zelditch, J. Diff. Geom. **49** 207 (1998).
- [4] B. Gutkin and U. Smilansky J. Phys A.**31**, 6061-6068 (2001).
- [5] S. Zelditch “Survey on the inverse spectral problem” to appear in J. Diff. Geom. Surveys (2004).
- [6] J. Milnor Proc. Nat. Acad. Sci. USA, **51** (1964), 542.
- [7] M. E. Fisher, J. Combinatorial Theory J. Combinatorial Theory **1** 105-125 (1966) .
- [8] C. Gordon, D. Webb and S . Wolpert, Bull. Am. Math. Soc. **27** 134-138 (1992).
- [9] S. Chapman Amer. Math. Mon. **102** (1995), 124.
- [10] T. Sunada, Ann. of math. **121** 196-186,(1985).
- [11] R. Brooks, Ann. Inst. Fourier **49** 707-725,(1999).
- [12] A. Schiemann, Arch. Math. **54** (1990), 372.
- [13] P. Buser, J. Conway, P. Doyle and K.-D. Semmler, Int. Math. Res. Notices **9** (1994), 391-400.
- [14] Y. Okada and A. Shudo J. Phys. A: Math. Gen. **34** 5911-5922 (2001).
- [15] M. Kneser Math. Ann. **118**(1967) 31.
- [16] S. Wolpert Trans. Am. Math. Soc. **244** (1978), 313.
- [17] C. R. Earnest and G. Nipp, Math. Rep. Acad. Sci. Canada **13** (1991), 33.
- [18] J. H. Conway and N. J. A. Sloane, Duke Math. J. **66** (1992), 93.
- [19] J. W. S. Cassels, “Rational quadratic forms”, Academic Press, London, (1978)
- [20] H. Iwaniec “Topics in classical automorphic forms”, American Mathematical Society, (1997).
- [21] Z. Rudnick, private communication.
- [22] G. Blum, S. Gnutzmann and U. Smilansky, Phys. Rev. Lett. **88** 114101 (2002).
- [23] Galia Shapira and Uzy Smilansky “Quantum graphs which sound the same”, in preparation.